Sub-inertial dynamics of density-driven flows in a continuously stratified fluid on a sloping bottom. I. Model derivation and stability characteristics

BY FRANCIS J. POULIN AND GORDON E. SWATERS

Applied Mathematics Institute, Department of Mathematical Sciences, University of Alberta, Edmonton, Alberta, Canada T6G 2G1

A theory is developed describing the sub-inertial baroclinic dynamics of bottom-intensified density-driven flows within a continuously stratified fluid of finite depth with variable bottom topography. The evolution of the density-driven current is modelled as a geostrophically balanced homogeneous flow, which allows for finite-amplitude dynamic thickness variations and for which the pressure fields in each layer are strongly coupled together. The evolution of the overlying fluid is governed by baroclinic quasi-geostrophic dynamics describing a balance between the production of relative vorticity, the vortex-tube stretching/compression associated with a deforming gravity current height, and the rectifying influence of a background topographic vorticity gradient. The model is derived as a systematic asymptotic reduction of the two-fluid system in which the upper fluid is described by the Boussinesq adiabatic equations for a continuously stratified fluid and a lower homogeneous layer described by shallow-water theory appropriate for an f-plane with variable bottom topography. The model is shown to possess a non-canonical Hamiltonian formulation. This structure is exploited to give a variational principle for arbitrary steady solutions and stability conditions in the sense of Liapunov.

The general linear stability problem associated with parallel shear flow solutions is examined in some detail. Necessary conditions for instability are derived. The instability is convective in the sense that it proceeds by extracting the available gravitational potential energy associated with the lower-layer water mass sliding down the sloping bottom. For the normal-mode instability problem, a semicircle theorem is derived. The linear stability characteristics are illustrated by solving the normal-mode equations for a simple linearly varying lower-layer height profile. In the overlying fluid, the unstable normal modes correspond to amplifying bottom-intensified topographic Rossby waves.

Keywords: gravity currents; density-driven currents;
fronts; physical oceanography

1. Introduction and model derivation

The continental shelf regions of the world's oceans provide an important wave and flow guide. In addition to allowing for the along-coast propagation of large-scale waves

such as continental shelf, Poincaré and Kelvin waves, among others, the ambient slop-
ing bottom topography permits the along-slope flow of bottom-intensified density
currents. These baroclinic flows arise as a geostrophic balance between the gravity-
driven down-slope acceleration of a relatively dense water mass sitting directly on
a sloping bottom and the Coriolis effect, which deflects the motion to the along-
slope direction (toward the right in the Northern Hemisphere). To emphasize the
underlying dynamics (e.g. the horizontal length-scale is on the order of the defor-
mation radius), and to differentiate them from their non-rotating counterparts (see,
for example, Britter & Linden 1980), we refer to these flows as *mesoscale gravity
currents*.

The flows associated with the coastal transport of deep and bottom waters are
mesoscale gravity currents. Examples include the Denmark Strait overflow (Smith
1976; Bruce 1995), the initial migration of Antarctic bottom water (Whitehead &
Worthington 1982), density intrusions in the Adriatic Sea (Zoccolotti & Salusti 1987),
deep-water exchange in the Strait of Georgia (LeBlond *et al.* 1991) and benthic cur-
rents along the New England Shelf (see, for example, Houghton *et al.* 1982), among
many others. These flows form a critical component of the oceanic thermohaline cir-
culation and, consequently, play a major role in the Earth's evolving climate (see,
for example, Price & Baringer 1994; Jiang & Garwood 1996).

The principal purpose of this paper is to present a theory describing the dynamics
of these flows, paying particular attention to their baroclinic interaction with the sur-
rounding stratified ocean. This paper focuses on the model formulation and provides
a detailed description of the linear and nonlinear stability characteristics of mesoscale
gravity currents exploiting the underlying Hamiltonian structure and normal-mode
instability equations. In Poulin & Swaters (1999*a*, hereafter referred to as part II), we
focus on describing the properties of isolated-eddy and radiating-cold-dome solutions
of the model.

Early descriptions of mesoscale gravity currents were based on streamtube models
(see, for example, Smith 1975; Killworth 1977; Melling & Lewis 1982). While these
models were able to provide reasonable estimates for certain averaged flow quanti-
ties, they were unable to describe the along-slope spatial and temporal development
of these flows. Griffiths *et al.* (1982; hereafter referred to as GKS) presented a lin-
ear stability analysis using a reduced gravity model of gravity-driven currents on a
sloping bottom and compared their theoretical results to rotating tank experiments
of the instability of buoyancy-driven, i.e. surface-intensified, currents. There were
several differences between GKS's theoretical stability results and the laboratory
simulations, and these were attributed, in part, to the presence of an unstable baro-
clinic mode outside the applicability of their analysis. Other studies of the theoretical
description of density-driven gravity currents include Speer *et al.* (1993) and Shapiro
& Hill (1997).

There is another phenomenological difference between the instability of mesoscale
gravity currents on a sloping bottom and surface buoyancy-driven currents that
is worth emphasizing. As a number of numerical simulations (see, for example,
Gawarkiewicz & Chapman 1995; Chapman & Gawarkiewicz 1995; Jiang & Gar-
wood 1995, 1996) have made clear, the spatial structure of the baroclinic instabilities
associated with density-driven flows on a sloping bottom are strongly asymmetri-
cal in the cross-slope direction, in contrast to those associated with surface-driven
currents.

The asymmetry is the result of the fact that the baroclinic instability of a mesoscale gravity current is driven by the release of the available gravitational potential energy associated with having a pool of relatively dense water sitting directly on a sloping bottom. The energy is released through the formation of down-slope-propagating plumes on the down-slope edge of the current. This results in the preferential amplification of the perturbations on the down-slope side of the mesoscale gravity current compared to those on the up-slope side.

There is no analogous preferential amplification of the perturbations to the boundaries of surface-driven currents (on an f-plane) because there is no external force acting to break the underlying cross-current symmetry. Thus, for buoyancy-driven surface currents, the unstable modes have the usual symmetries associated with varicose or sinuous perturbations. This helps to explain, in part, the discrepancy between the theoretical predictions and the laboratory experiments described by GKS.

The asymmetrical spatial structure of the baroclinic instabilities was a property of the instability theory presented by Swaters (1991). In that paper, a model for the baroclinic evolution of density-driven currents was derived, based on a sub-inertial asymptotic reduction of the two-layer shallow-water equations on an f-plane with variable topography, which allowed for finite-amplitude thickness variations in the density-driven current, while filtering out barotropic instabilities. The overlying layer, or surrounding slope water, was described by quasi-geostrophic (QG) dynamics, which incorporated the generation of relative vorticity by vortex stretching/compression associated with the deforming interface between the density-driven current and the slope water and the background vorticity gradient associated with the bottom slope. The instability mechanism identified by Swaters (1991) has been described as the process responsible for the destabilization of density-driven currents in numerical simulations (Jiang & Garwood 1996).

The Swaters (1991) model showed that the growth rates and wavelengths of the most unstable mode depended on various environmental parameters, such as the bottom slope and initial current height (see, for example, Karsten *et al.* 1995). Perhaps the most significant shortcoming of the Swaters model is that it does not retain any stratification in the overlying slope water.

It is reasonable to expect that retaining stratification in the overlying water will lead to modifications in the predicted growth rates and spatial characteristics of the instabilities. We will show that the growth rate and wavenumber of the most unstable mode increases with increasing Brunt–Väisälä frequency associated with the overlying slope water. This result is particularly important for the applications we are interested in. For example, the application of the Swaters (1991) instability model by Karsten *et al.* (1995) describing the destabilization of the deep-water renewal current in the Strait of Georgia gave a typical result for the wavelength of the most unstable mode, which was about twice as large as the horizontal length-scale obtained for the observed sub-surface eddies (see, for example, Steacy *et al.* 1988).

Another principal effect that stratification will have on the solutions we discuss here and in part II will be, of course, their vertical structure. Numerical simulations (see, for example, Gawarkiewicz & Chapman 1995; Chapman & Gawarkiewicz 1995; Jiang & Garwood 1995, 1996) clearly indicate (as do oceanographic observations, e.g. Steacy *et al.* (1988)) that the instabilities are bottom intensified. It is of interest, therefore, to build on the success of the dynamical balances in the Swaters (1991) theory, and to develop a new model that describes, perhaps somewhat more

accurately, the vertical structure seen in numerical simulations, oceanographic obser-
vations and recent laboratory experiments (Honji & Hosoyamada 1989; P. Baines,
personal communication; D. Etling, personal communication).

The plan of this paper is as follows. In the remainder of this section we derive the
model via a suitable asymptotic reduction of a two-fluid coupled system on an f-
plane in which the upper fluid is initially described by the stratified, incompressible
and adiabatic fluid equations, and the lower fluid, i.e. the density-driven current, is
described by the shallow-water equations with variable bottom topography.

In §2, we briefly describe the underlying Hamiltonian formulation of the model
(complete details can be found in Poulin (1997)) and use this structure to estab-
lish linear and nonlinear stability criteria in the sense of Liapunov (see also Poulin
& Swaters 1999b). In §3, we analyse in some detail the general and normal-mode
linear instability problem. Several general results are presented, including necessary
mass flux conditions for instability and a semicircle theorem. We illustrate the insta-
bility characteristics by solving the linear instability problem corresponding to a
simple unsheared mesoscale gravity current in which the cross-slope thickness profile
is linear and does not possess incroppings. Although far too simple to have any real
applicability, the fact that this problem can be solved exactly permits us to illus-
trate, quite effectively, most of the qualitative features implicit in the instability. The
conclusions are given in §4.

(a) Governing equations

The underlying geometry is sketched in figure 1. We assume f-plane dynamics with
a stably stratified fluid of finite depth overlying a homogeneous fluid with variable
bottom topography. The upper, i.e. the continuously stratified, layer is denoted as
layer 1. The gravity current, i.e. the lower layer, is denoted as layer 2. The upper-
and lower-layer dynamical quantities will be denoted, unless otherwise specified, by
subscripts 1 and 2, respectively.

The theoretical work starts with the incompressible adiabatic equations under a
Boussinesq approximation for a continuously stratified fluid for the upper layer, and
the shallow-water equations for the lower layer. We assume a rigid upper surface for
the upper layer, which will filter out the external gravity wave modes in the model.

The idea here is to derive a model that focuses on the baroclinic aspects of the
problem and filters out barotropic processes, while respecting the kinematic prop-
erty that the appropriate scaling for the *dynamic* deflections of the lower layer is a
representative height of the lower layer itself (see figure 1), since we wish to develop
a model that can describe coupled fronts or isolated eddies with the property that
the scale of the dynamic variations of the lower-layer fluid height is similar to the
lower-layer thickness scale itself.

This assumption will imply that one cannot neglect, to leading order, the space/
time gradients in the height of the cold pool or gravity current in the continuity
equation for the lower layer (as one does in QG theory). However, in accordance with
the available data, we assume that the velocities in the two layers are geostrophically
determined. The two layers will be strongly coupled together, in the sense that the
reduced pressures in each layer cannot be decoupled from each other even at leading
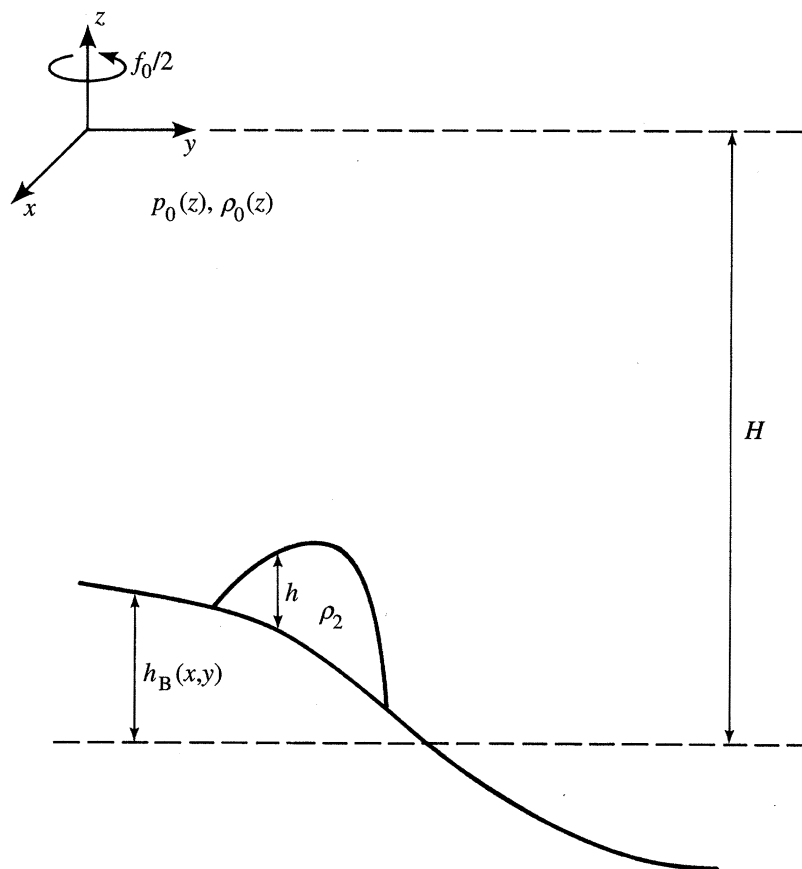order.

Figure 1. Geometry of the model used in this paper.

The *dimensional* equations of motion in the upper layer are given by

$$(\partial_{t^*} + \boldsymbol{u}_1^* \cdot \nabla^* + w^* \partial_{z^*}) \boldsymbol{u}_1^* + f\boldsymbol{e}_3 \times \boldsymbol{u}_1^* = -(1/\rho_2)\nabla^* p_1^*, \tag{1.1}$$

$$\rho_2(\partial_{t^*} + \boldsymbol{u}_1^* \cdot \nabla^* + w^* \partial_{z^*}) w^* = -\partial_{z^*} p_1^* - g\rho^*, \tag{1.2}$$

$$\nabla^* \cdot \boldsymbol{u}_1^* + w_{z^*}^* = 0, \tag{1.3}$$

$$(\partial_{t^*} + \boldsymbol{u}_1^* \cdot \nabla^* + w^* \partial_{z^*})\rho^* = 0, \tag{1.4}$$

where $\boldsymbol{u}_1^* = (u_1^*, v_1^*)$, w^*, ρ_2, p_1^*, $\nabla^* = (\partial_{x^*}, \partial_{y^*})$ and ρ^* are, respectively, the upper-layer horizontal velocity field, vertical velocity, constant reference Boussinesq density (which we take to be the density of the lower layer denoted as ρ_2), total pressure field, the horizontal gradient operator, and the variable density field in the upper layer. The notation is standard and alphabetical subscripts indicate partial differentiation unless otherwise indicated.

The lower layer is assumed to be governed by shallow-water theory. The *dimensional* governing equations are given by

$$(\partial_{t^*} + \boldsymbol{u}_2^* \cdot \nabla^*)\boldsymbol{u}_2^* + f\boldsymbol{e}_3 \times \boldsymbol{u}_2^* = -(1/\rho_2)\nabla^* p^*, \tag{1.5}$$

$$h_{t^*}^* + \nabla^* \cdot (\boldsymbol{u}_2^* h^*) = 0, \tag{1.6}$$

where $\boldsymbol{u}_2^* = (u_2^*, v_2^*)$, p^* and h^* are, respectively, the lower-layer horizontal velocity, the dynamic pressure and thickness, or current height relative to the bottom topography.

(i) *Boundary conditions*

Assuming a rigid upper surface, the *dimensional* kinematic vertical boundary conditions associated with the upper layer are given by

$$
\left.\begin{array}{ll}
w^* = 0, & \text{on } z^* = 0, \\
w^* = (\partial_{t^*} + \boldsymbol{u}_1^* \cdot \nabla^*)[h^* + h_B^*], & \text{on } z^* = -H + h^* + h_B^*,
\end{array}\right\} \tag{1.7}
$$

respectively, where H and $h_B^* = h_B^*(x^*, y^*)$ are the reference depth of the upper layer and the height of the variable bottom topography, respectively. The slopes associated with the bottom topography are assumed to be small enough so as to not violate the hydrostatic approximation that is implicit in deriving the shallow-water equations (1.5) and (1.6).

It will eventually be necessary to Taylor expand the kinematic boundary condition at $z^* = -H + h^* + h_B^*$ about $z^* = -H$. To leading order, we have

$$
w^* = (\partial_{t^*} + \boldsymbol{u}_1^* \cdot \nabla^*)[h^* + h_B^*] + O\left[w^*\left(\frac{h^*}{H}, \frac{h_B^*}{H}\right)\right], \quad \text{on } z^* = -H. \tag{1.8}
$$

We note that the assumptions that are being made in this and the subsequent Taylor expansion for the kinematic and dynamic boundary conditions at $z^* = -H + h^* + h_B^*$ are exactly analogous to the usual assumptions of QG theory for a continuously stratified fluid with variable topography, i.e. the bottom is gently sloping and the height of the lower layer is small in comparison with the scale depth of the upper layer (see, for example, LeBlond & Mysak 1978).

The dynamic boundary condition across the two layers is that the total pressure be continuous across the interface. If we denote the background hydrostatic density field in the upper layer as $\rho_0(z^*)$ and the *total* pressure field in the lower layer as $p_2^*(x^*, y^*, z^*, t^*)$, it is convenient to write p_1^* and p_2^* in the form

$$
p_1^*(x^*, y^*, z^*, t^*) = g \iint_{z^*}^{0} \rho_0(\xi)\, \mathrm{d}\xi + \varphi^*(x^*, y^*, z^*, t^*), \tag{1.9}
$$

$$
p_2^*(x^*, y^*, z^*, t^*) = g \iint_{-H}^{0} \rho_0(\xi)\, \mathrm{d}\xi - g\rho_2(z^* + H) + p^*(x^*, y^*, t^*), \tag{1.10}
$$

where $\varphi^*(x^*, y^*, z^*, t^*)$ is the dimensional reduced pressure in the upper layer.

Pressure continuity across the interface $z^* = -H + h^* + h_B^*$ is, therefore, satisfied provided

$$
g \iint_{-H+h^*+h_B^*}^{0} \rho_0(\xi)\, \mathrm{d}\xi + \varphi^*(x^*, y^*, -H + h^* + h_B^*, t^*)
$$

$$
= g \iint_{-H}^{0} \rho_0(\xi)\, \mathrm{d}\xi - g\rho_2(h^* + h_B^*) + p^*(x^*, y^*, t^*). \tag{1.11}
$$

It will become necessary to Taylor expand the first integral in (1.11) about $z^* = -H$. To leading order, we have

$$
-g\rho_0(-H)(h^* + h_B^*) + \varphi^* \,|_{z^*=-H} = -g\rho_2(h^* + h_B^*) + p^* + \cdots, \tag{1.12}
$$

which can be rewritten in the form

$$
p^* = \varphi^* + g'\rho_2(h^* + h_B^*) + \cdots, \quad \text{on } z^* = -H, \tag{1.13}
$$

where the reduced gravity g' is given by

$$
g' = [(g(\rho_2 - \rho_0(-H)))/\rho_2] > 0. \tag{1.14}
$$

We will describe any horizontal boundary conditions as the need arises.

(ii) *Scalings and non-dimensional equations*

Our approach to developing the non-dimensional equations is to introduce a straightforward modification and extension of the arguments advanced in Swaters & Flierl (1991) and Swaters (1991). We scale the lower-layer velocity field with the *Nof speed* $g's^*/f$, where s^* is a representative slope associated with the bottom topography. The reason for this choice is that, in the absence of any dynamic interaction between the two layers (i.e. a reduced-gravity model), Nof (1983) has shown that this is the propagation speed of any compactly supported cold eddy.

The horizontal length-scale, denoted by L, is the internal deformation radius associated with the upper layer given by

$$L = \sqrt{g'H}/f.$$

We remark that this is an intermediate length-scale that is larger than the internal deformation radius associated with the lower layer. This is the appropriate length-scale if the essential nonlinearity in the problem occurs not in the momentum equations but in the continuity equation (see, for example, Charney & Flierl 1981). Given this length-scale, we assume that time is scaled advectively.

The horizontal velocity field in the upper layer is scaled assuming that it is principally generated by vortex-tube stretching associated with a deforming interface, i.e.

$$e_3 \cdot (\nabla \times u_1^*) \simeq O(fh^*/H).$$

The vertical velocity in the upper layer is scaled so that

$$w^* \simeq O(h_{t^*}^*),$$

which is consistent with (1.8). The dynamic pressure field in each layer is scaled geostrophically, and the dynamic density field in the upper layer is scaled so that it is in hydrostatic balance with the upper-layer dynamic pressure field.

The non-dimensional variables, which do not have an asterisk associated with them, are related to the dimensional variables through the relations

$$u_2^* = (g's^*/f)u_2, \qquad p^* = \rho_2 g's^* Lp, \qquad h^* = h_0 h, \qquad (1.15)$$

$$h_B^* = s^* Lh_B, \qquad (x^*, y^*) = L(x, y), \qquad z^* = Hz, \qquad (1.16)$$

$$t^* = \left(\frac{fL}{g's^*}\right)t, \qquad u_1^* = \delta Lf u_1, \qquad w^* = \left(\frac{g's^* h_0}{fL}\right)w, \qquad (1.17)$$

$$p_1^* = g \iint_{z^*}^0 \rho_0(\xi)\,d\xi + \rho_2 \delta(fL)^2 \varphi(x, y, z, t), \qquad (1.18)$$

$$\rho^* = \rho_0(z^*) + \left(\frac{\rho_2 \delta(fL)^2}{gH}\right)\rho, \qquad (1.19)$$

where h_0 is a representative scaling for the lower-layer thickness or height, and the parameter δ is given by

$$\delta \equiv h_0/H. \qquad (1.20)$$

Substitution of (1.15)–(1.20) into the dimensional equations leads to

$$s(\partial_t + [\delta/s]\boldsymbol{u}_1 \cdot \nabla + \delta w \partial_z)\boldsymbol{u}_1 + \boldsymbol{e}_3 \times \boldsymbol{u}_1 + \nabla\varphi = \boldsymbol{0}, \tag{1.21}$$

$$\left(\frac{sH}{L}\right)^2 \left(\partial_t + \frac{\delta}{s}\boldsymbol{u}_1 \cdot \nabla + \delta w \partial_z\right)w + \rho + \varphi_z = 0, \tag{1.22}$$

$$\nabla \cdot \boldsymbol{u}_1 + s w_z = 0, \tag{1.23}$$

$$(\partial_t + [\delta/s]\boldsymbol{u}_1 \cdot \nabla)\rho + \delta w \rho_z = N^2(z)w, \tag{1.24}$$

$$s(\partial_t + \boldsymbol{u}_2 \cdot \nabla)\boldsymbol{u}_2 + \boldsymbol{e}_3 \times \boldsymbol{u}_2 + \nabla p = \boldsymbol{0}, \tag{1.25}$$

$$h_t + \nabla \cdot (\boldsymbol{u}_2 h) = 0, \tag{1.26}$$

where s is the scaled slope parameter given by

$$s \equiv \frac{s^* L}{H} \equiv \frac{s^* g'/f}{\sqrt{g'H}}, \tag{1.27}$$

and the non-dimensional Brunt–Väisälä frequency, denoted by $N(z)$, is determined by

$$N^2(z) = -\frac{H}{\rho_2 - \rho_0(H)} \left[\frac{\mathrm{d}\rho_0(z^*)}{\mathrm{d}z^*}\right]_{z^*=Hz} > 0, \tag{1.28}$$

and we assume the aspect ratio satisfies $(H/L) < 1$.

The parameter s, which is a scaled bottom-slope parameter, may be interpreted as the ratio of the (rotationally dominant) Nof speed to a non-rotating gravity current speed. Another point to emphasize once again is that the continuity equation for the gravity current, i.e. (1.26), is fully nonlinear to leading order, that is, the scale amplitude for the dynamic deflections of the gravity current height is of the same order as the scale thickness itself.

The non-dimensional vertical boundary conditions are given by

$$w = 0, \qquad\qquad \text{on } z = 0, \tag{1.29}$$

$$w = h_t + \boldsymbol{u}_1 \cdot \nabla(h_\mathrm{B} + [\delta/s]h) + O(s,\delta), \qquad \text{on } z = -1, \tag{1.30}$$

$$p = h_\mathrm{B} + [\delta/s](\varphi + h) + O(s,\delta), \qquad\qquad \text{on } z = -1. \tag{1.31}$$

Typical mesoscale density-driven flows on continental slopes satisfy (see, for example, Swaters & Flierl 1991)

$$\delta \simeq O(s), \quad \text{with } 0 < s \ll 1. \tag{1.32}$$

It is convenient to introduce the parameter μ defined by

$$\delta = \mu s, \quad \text{with } \mu \simeq O(1), \tag{1.33}$$

into the non-dimensional equations, yielding

$$s(\partial_t + \mu\boldsymbol{u}_1 \cdot \nabla + s\mu w \partial_z)\boldsymbol{u}_1 + \boldsymbol{e}_3 \times \boldsymbol{u}_1 + \nabla\varphi = \boldsymbol{0}, \tag{1.34}$$

$$(sH/L)^2(\partial_t + \mu\boldsymbol{u}_1 \cdot \nabla + s\mu w \partial_z)w + \rho + \varphi_z = 0, \tag{1.35}$$

$$\nabla \cdot \boldsymbol{u}_1 + s w_z = 0, \tag{1.36}$$

$$(\partial_t + \mu\boldsymbol{u}_1 \cdot \nabla)\rho + s\mu w \rho_z = N^2(z)w, \tag{1.37}$$

$$s(\partial_t + \boldsymbol{u}_2 \cdot \nabla)\boldsymbol{u}_2 + \boldsymbol{e}_3 \times \boldsymbol{u}_2 + \nabla p = \boldsymbol{0}, \tag{1.38}$$

$$h_t + \nabla \cdot (\boldsymbol{u}_2 h) = 0, \tag{1.39}$$

with the vertical boundary conditions

$$w = 0, \qquad\qquad\qquad\qquad \text{on } z = 0, \qquad (1.40)$$

$$w = h_t + \boldsymbol{u}_1 \cdot \nabla(h_\mathrm{B} + \mu h) + O(s), \quad \text{on } z = -1, \qquad (1.41)$$

$$p = h_\mathrm{B} + \mu(\varphi + h) + O(s), \qquad \text{on } z = -1. \qquad (1.42)$$

The parameter μ, which we call the interaction parameter, may be interpreted as measuring (as it turns out) the ratio of the destabilizing effect of baroclinicity to the stabilizing effect of topography.

The non-dimensional equations are now in the form in which we can rationally introduce an asymptotic expansion with respect to the small parameter s. Notice that the position of the parameter s in (1.34)–(1.37) occurs in exactly the same manner as the Rossby number in classical QG theory for a continuously stratified fluid (see, for example, Pedlosky 1987).

Thus, if we introduce the straightforward asymptotic expansion

$$(\boldsymbol{u}_1, w, \boldsymbol{u}_2, \varphi, p, h) \simeq (\boldsymbol{u}_1, w, \boldsymbol{u}_2, \varphi, p, h)^{(0)} + s(\boldsymbol{u}_1, w, \boldsymbol{u}_2, \varphi, p, h)^{(1)} + \cdots, \qquad (1.43)$$

into the governing equations, the leading-order fields will be determined by

$$\partial_t [\triangle\varphi^{(0)} + (N^{-2}\varphi_z^{(0)})_z] + \mu J(\varphi^{(0)}, \triangle\varphi^{(0)} + (N^{-2}\varphi_z^{(0)})_z) = 0, \qquad (1.44)$$

with the vertical boundary conditions

$$\varphi_{zt}^{(0)} + \mu J(\varphi^{(0)}, \varphi_z^{(0)}) = 0, \quad \text{on } z = 0, \qquad (1.45)$$

$$\varphi_{zt}^{(0)} + \mu J(\varphi^{(0)}, \varphi_z^{(0)}) + N^2 J(\varphi^{(0)} + h^{(0)}, h_\mathrm{B}) = 0, \quad \text{on } z = -1, \qquad (1.46)$$

$$h_t^{(0)} + J(\mu\varphi^{(0)} + h_\mathrm{B}, h^{(0)}) = 0, \quad \text{on } z = -1, \qquad (1.47)$$

where the other leading-order fields are determined by

$$\rho^{(0)} = -\varphi_z^{(0)}, \qquad (1.48)$$

$$w^{(0)} = -N^{-2}[\varphi_{zt}^{(0)} + \mu J(\varphi^{(0)}, \varphi_z^{(0)})], \qquad (1.49)$$

$$\boldsymbol{u}_1^{(0)} = \boldsymbol{e}_3 \times \nabla\varphi^{(0)}, \qquad (1.50)$$

$$\boldsymbol{u}_2^{(0)} = \boldsymbol{e}_3 \times \nabla[h_\mathrm{B} + \mu(\varphi^{(0)}\,|_{z=-1} + h^{(0)})], \qquad (1.51)$$

$$p^{(0)} = h_\mathrm{B} + \mu(\varphi^{(0)}\,|_{z=-1} + h^{(0)}), \qquad (1.52)$$

where the Jacobian is given by $J(A, B) = A_x B_y - A_y B_x$.

The governing equations for the upper layer are like baroclinic QG theory, except that the bottom boundary condition is replaced with a pair of partial differential equations that couple the evolution of $\varphi_z^{(0)}$ at $z = -1$ to the evolution of the lower-layer height $h^{(0)}$.

Equation (1.47) can be thought of as either the mass-conservation equation for a geostrophically balanced flow on a sloping bottom, or as $-(h^{(0)})^2$ times the leading-order potential-vorticity equation for the lower layer, since, for the asymptotic limit examined here, the lower-layer potential vorticity, denoted by PV_2, is given by $\mathrm{PV}_2 \simeq 1/h^{(0)}$ to leading order in s.

In fact, one can interpret the asymptotic limit used in the lower layer as corresponding to a planetary geostrophic (see, for example, Pedlosky 1984) balance, in which the background vorticity gradient is given by the local topographic slope.

However, as we show in §3, our model does not exhibit an ultraviolet catastrophe in the instability problem (as is known to occur in some planetary geostrophic models; see, for example, de Verdiere (1986)). Since we are only going to work in what follows with the leading-order equations (1.44)–(1.52), we will, henceforth, drop the (0)-superscript.

2. Hamiltonian structure, variational principle and stability conditions

(a) Hamiltonian formulation of the model

A system of n partial differential equations written abstractly in the form

$$\Phi\left(\boldsymbol{q}, \frac{\partial}{\partial x_i}, \frac{\partial}{\partial t}\right) = \boldsymbol{0}, \tag{2.1}$$

where t is time and

$$\boldsymbol{q}(\boldsymbol{x}, t) = (q_1(\boldsymbol{x}, t), \dots, q_n(\boldsymbol{x}, t))^{\mathrm{T}}$$

is a column vector of n dependent variables, with the m independent spatial variables $\boldsymbol{x} = (x_1, \dots, x_{\mathrm{m}})$ defined on the open spatial domain $\Omega \subseteq \mathbb{R}^m$ with the boundary (if it exists) $\partial\Omega$, is said to be Hamiltonian (see, for example, Olver 1982; Benjamin 1984) if there exists a conserved functional $H(\boldsymbol{q})$, called the Hamiltonian, and a matrix $\mathcal{M}$ of (possibly pseudo-) differential operators (the cosymplectic form), such that (2.1) can be written in the form

$$\boldsymbol{q}_t = \mathcal{M}\frac{\delta H}{\delta \boldsymbol{q}}, \tag{2.2}$$

where $\delta H/\delta \boldsymbol{q}$ is the vector variational, or Euler–Lagrange derivative, of H with respect to $\boldsymbol{q}$, and where the Poisson bracket defined by (see, for example, Morrison 1982)

$$[F, G] \equiv \left\langle \frac{\delta F}{\delta \boldsymbol{q}}, \mathcal{M}\frac{\delta G}{\delta \boldsymbol{q}} \right\rangle, \tag{2.3}$$

where F and G are arbitrary smooth functionals of $\boldsymbol{q}$, and $\langle *_1, *_2 \rangle$ is the inner product, satisfies the algebraic properties of skew symmetry, distributive and associative laws and the Jacobi identity.

The Hamiltonian formulation is singular if the Poisson bracket is degenerate, that is, if there are non-trivial functionals that satisfy

$$\mathcal{M}\frac{\delta C}{\delta \boldsymbol{q}} = \boldsymbol{0}. \tag{2.4}$$

The non-trivial solutions $C = C(\boldsymbol{q})$ are the time-invariant Casimir functionals. These are important since, as it turns out, they are necessary in order to construct a variational principle for steady or steadily travelling eddy solutions to the model equations.

It follows from (2.2) and (2.3) that we may write the system of partial differential equations alternatively in the form

$$\boldsymbol{q}_t = [\boldsymbol{q}, H], \tag{2.5}$$

provided we interpret $\delta \boldsymbol{q}/\delta \boldsymbol{q}$ as the appropriate matrix of delta functions.

The model equations (1.44)–(1.47) may be written in the form

$$\partial_t[\triangle\varphi + (N^{-2}\varphi_z)_z] + \mu J(\varphi, \triangle\varphi + (N^{-2}\varphi_z)_z) = 0, \tag{2.6}$$

$$\varphi_{zt} + \mu J(\varphi, \varphi_z) = 0, \quad \text{on } z = 0, \tag{2.7}$$

$$\partial_t[\varphi_z + N^2(h + h_\text{B}/\mu)] + \mu J(\varphi, \varphi_z + N^2(h + h_\text{B}/\mu)) = 0, \quad \text{on } z = -1, \tag{2.8}$$

$$h_t + J(\mu\varphi + h_\text{B}, h) = 0, \quad \text{on } z = -1, \tag{2.9}$$

where (2.8) is obtained by forming the sum $(1.46) + N^2(1.47)$.

It is necessary to be clear about the domain and boundary conditions. For the purposes of this section, we take the simplest configuration and assume a simply connected domain, denoted by Ω, given by

$$\Omega = (-1, 0) \times \Omega_\text{H},$$

where Ω_H is the horizontal component of the domain with boundary denoted $\partial\Omega_\text{H}$. Since we assume here that the domain is simply connected, it follows that we may choose, without loss of generality, $\varphi = 0$ on $\partial\Omega_\text{H}$.†

The Hamiltonian structure for our model is a blend of that for the continuously stratified QG equations (Holm 1985) and the Swaters (1991) model (Swaters 1993). The system of equations (2.6)–(2.9) is Hamiltonian for the choice of

$$H(\boldsymbol{q}) = \tfrac{1}{2}\mu \iiint_\Omega \nabla\varphi \cdot \nabla\varphi + (\varphi_z/N)^2 \,\mathrm{d}x\mathrm{d}y\mathrm{d}z$$

$$+ \tfrac{1}{2}\mu \iint_{\Omega_\text{H}} (h + h_\text{B}/\mu)^2 - (h_\text{B}/\mu)^2 \,\mathrm{d}x\mathrm{d}y, \tag{2.10}$$

$$\boldsymbol{q} = (q_1, q_2, q_3, q_4)^\text{T}, \tag{2.11}$$

where

$$q_1 = \triangle\varphi + (N^{-2}\varphi_z)_z, \qquad\qquad q_2 = \varphi_z\,|_{z=0}, \tag{2.12}$$

$$q_3 = \varphi_z\,|_{z=-1} + N^2(-1)(h + h_\text{B}/\mu), \qquad q_4 = h, \tag{2.13}$$

with the Poisson bracket

$$[F, G] = \iiint_\Omega \frac{\delta F}{\delta q_1} J\left(\frac{\delta G}{\delta q_1}, q_1\right) \mathrm{d}x\mathrm{d}y\mathrm{d}z - \iint_{\Omega_\text{H}} \left[N^2 \frac{\delta F}{\delta q_2} J\left(\frac{\delta G}{\delta q_2}, q_2\right)\right]_{z=0} \mathrm{d}x\mathrm{d}y$$

$$+ \iint_{\Omega_\text{H}} \left[N^2 \frac{\delta F}{\delta q_3} J\left(\frac{\delta G}{\delta q_3}, q_3\right)\right]_{z=-1} \mathrm{d}x\mathrm{d}y - \iint_{\Omega_\text{H}} \frac{\delta F}{\delta q_4} J\left(\frac{\delta G}{\delta q_4}, q_4\right) \mathrm{d}x\mathrm{d}y. \tag{2.14}$$

From (2.14) we conclude that the cosymplectic form is given by

$$\mathcal{M} = \begin{bmatrix} J(*, q_1) & 0 & 0 & 0 \\ 0 & -N^2(0)J(*, q_2) & 0 & 0 \\ 0 & 0 & N^2(-1)J(*, q_3) & 0 \\ 0 & 0 & 0 & -J(*, q_4) \end{bmatrix}, \tag{2.15}$$

---

† It is important to emphasize that other domains and boundary conditions, e.g. non-simply-connected domains, periodic channels, unbounded domains, etc., can be easily dealt with (see, for example, Shepherd 1990).

and, thus, the Casimirs are given by

$$C(\boldsymbol{q}) = \iiint_\Omega \Phi_1(q_1)\,\mathrm{d}x\mathrm{d}y\mathrm{d}z + \iint_{\Omega_H} \Phi_2(q_2) + \Phi_3(q_3) + \Phi_4(q_4)\,\mathrm{d}x\mathrm{d}y, \qquad (2.16)$$

where Φ_1, Φ_2, Φ_3 and Φ_4 are arbitrary differentiable functions of their arguments.

It is a lengthy but straightforward calculation to verify that the above structure is indeed a proper Hamiltonian formulation for the model equations. The proof is a blend of the arguments presented in Holm (1985) for the continuously stratified QG equations and for the Swaters (1991) two-layer model (Swaters 1993). Complete details can be found in Poulin (1997). Additional remarks can be found also in Poulin & Swaters (1999b).

(b) *Variational principle for steady solutions*

Let $\varphi_0(x, y, z)$ and $h_0(x, y)$ denote an arbitrary steady-state solution of (2.6)–(2.9); it follows that

$$J(\mu\varphi_0, \triangle\varphi_0 + (\varphi_{0_z}/N^2)_z) = 0, \qquad (2.17)$$

$$J(\mu\varphi_0, \varphi_{0_z}) = 0, \quad \text{on } z = 0, \qquad (2.18)$$

$$J(\mu\varphi_0, \varphi_{0_z} + N^2(h_0 + [h_B/\mu])) = 0, \quad \text{on } z = -1, \qquad (2.19)$$

$$J(\mu\varphi_0 + h_B, h_0) = 0, \quad \text{on } z = -1, \qquad (2.20)$$

which imply

$$\mu\varphi_0 = F_1(\triangle\varphi_0 + (\varphi_{0_z}/N^2)_z), \qquad (2.21)$$

$$\mu\varphi_0 = F_2(\varphi_{0_z}), \quad \text{on } z = 0, \qquad (2.22)$$

$$\mu\varphi_0 = F_3(\varphi_{0_z} + N^2(h_0 + [h_B/\mu])), \quad \text{on } z = -1, \qquad (2.23)$$

$$\mu\varphi_0 + h_B = F_4(h_0), \quad \text{on } z = -1, \qquad (2.24)$$

where the F_i are arbitrary functions of their arguments (the possible dependency of F_1 on z has been suppressed).

These relations satisfy the first-order necessary conditions for an extremal of the constrained Hamiltonian,

$$\mathcal{H} = H + C, \qquad (2.25)$$

i.e.

$$\delta\mathcal{H}(\varphi_0, h_0) = 0, \qquad (2.26)$$

provided the Casimir densities are given by

$$\left.\begin{aligned}
\Phi_1(q_1) &= \iint_0^{q_1} F_1(\tau)\,\mathrm{d}\tau, \\[2mm]
\Phi_2(q_2) &= -N^{-2}(0) \iint_0^{q_2} F_2(\tau)\,\mathrm{d}\tau, \\[2mm]
\Phi_3(q_3) &= N^{-2}(-1) \iint_{N^2(-1)h_B/\mu}^{q_3} F_3(\tau)\,\mathrm{d}\tau, \\[2mm]
\Phi_4(q_4) &= -\iint_0^{q_4} F_4(\tau)\,\mathrm{d}\tau - \tfrac{1}{2}\mu q_4^2.
\end{aligned}\right\} \qquad (2.27)$$

(c) *Stability conditions and implications of Andrews's theorem*

The second variation of the constrained Hamiltonian $\mathcal{H}$ evaluated at the steady-state solution is

$$\delta^2\mathcal{H}(\varphi_0, h_0) = \iiint_\Omega \mu[\nabla(\delta\varphi) \cdot \nabla(\delta\varphi) + (\delta\varphi_z/N)^2] + F'_{10}[\delta q_1]^2 \, \mathrm{d}x\mathrm{d}y\mathrm{d}z$$

$$+ \iint_{\Omega_{\mathrm{H}}} F'_{30}[\delta q_3/N]^2_{z=-1} - F'_{20}[\delta q_2/N]^2_{z=0} - F'_{40}[\delta q_4]^2 \, \mathrm{d}x\mathrm{d}y, \quad (2.28)$$

where $F'_{i0} = \mathrm{d}F_i(q_{i0})/\mathrm{d}q_i$ for $i = 1, 2, 3, 4$. Henceforth, it will be assumed that i ranges from 1 to 4 unless otherwise stated.

It is straightforward to verify that $\delta^2\mathcal{H}(\varphi_0, h_0)$ is an invariant of the linear stability problem, obtained by substituting $\varphi = \varphi_0 + \delta\varphi$ and $h = h_0 + \delta h$ into (2.6)–(2.9) and neglecting the quadratic perturbation terms, given by

$$[\Delta\delta\varphi + (\delta\varphi_z/N^2)_z]_t + J(\mu\delta\varphi - F'_{10}\delta q_1, \Delta\varphi_0 + (\varphi_{0_z}/N^2)_z) = 0, \quad (2.29)$$

$$\delta\varphi_{zt} + J(\mu\delta\varphi - F'_{20}\delta q_2, \varphi_{0_z}) = 0, \quad \text{on } z = 0, \quad (2.30)$$

$$[\delta\varphi_z + N^2\delta h]_t + J(\mu\delta\varphi - F'_{30}\delta q_3, \varphi_{0_z} + N^2(h_0 + h_{\mathrm{B}})) = 0, \quad (2.31)$$

$$\delta h_t + J(\mu\delta\varphi - F'_{40}\delta q_4, h_0) = 0, \quad (2.32)$$

where (2.31) and (2.32) are evaluated on $z = -1$.

If $\delta^2\mathcal{H}(\varphi_0, h_0)$ is definite for all perturbations, then it can be shown that the mean flow is linearly stable in the sense of Liapunov. Clearly,

$$(-1)^{i+1} F'_{i0} \geqslant 0, \quad \forall i, \quad (2.33)$$

is sufficient to establish the linear stability of (φ_0, h_0) with respect to the perturbation norm

$$\|\delta \boldsymbol{q}\| = [\delta^2\mathcal{H}(\varphi_0, h_0)]^{1/2}.$$

This result, which ensures that $\delta^2\mathcal{H}(\varphi_0, h_0)$ is positive definite, is the analogue of Arnol'd's first stability theorem (see, for example, Holm *et al.* 1985) for our model equations. The conditions (2.33) are a straightforward union of the known formal stability results for the continuously stratified QG equations (Swaters 1985) and the two-layer analogue of the present model (Swaters 1993).

It is more useful to rewrite these conditions in terms of the steady along-slope velocity fields. If (2.21)–(2.24) are differentiated with respect to y, it follows that

$$F'_{10} = \frac{\mu U_0}{(\Delta U_0 + (U_{0_z}/N^2)_z)}, \quad (2.34)$$

$$F'_{20} = \frac{\mu U_0}{U_{0_z}}, \quad \text{on } z = 0, \quad (2.35)$$

$$F'_{30} = \frac{\mu U_0}{(U_{0_z} - N^2(h_{0_y} + h_{B_y}/\mu))}, \quad \text{on } z = -1, \quad (2.36)$$

$$F'_{40} = \frac{(h_{B_y} - \mu U_0)}{h_{0_y}}, \quad \text{on } z = -1, \quad (2.37)$$

where $U_0 = -\varphi_{0_y}$.

The stability conditions (2.33) are, therefore, equivalent to

$$\frac{U_0}{(\Delta U_0 + (U_{0_z}/N^2)_z)} \geqslant 0, \tag{2.38}$$

$$\frac{U_0}{U_{0_z}} \leqslant 0, \quad \text{on } z = 0, \tag{2.39}$$

$$\frac{U_0}{(U_{0_z} - N^2(h_{0_y} + h_{B_y}/\mu))} \geqslant 0, \quad \text{on } z = -1, \tag{2.40}$$

$$\frac{(\mu U_0 - h_{B_y})}{h_{0_y}} \geqslant 0, \quad \text{on } z = -1. \tag{2.41}$$

Clearly, these stability conditions correspond to a combination of Fjørtoft's stability criteria for the continuously stratified QG equations on an f-plane (see, for example, Pedlosky 1987, §7.3) and those obtained for the two-layer analogue of the present model (Swaters 1991).

We are particularly interested in focusing on the destabilization of a mesoscale gravity current, i.e. a configuration without an unstable mean flow profile in the overlying fluid. In the limit $\varphi_0 = 0$ and $h_0 = h_0(y)$, the above stability conditions reduce to simply

$$h_{B_y} h_{0_y} \leqslant 0.$$

Hence, a necessary condition for instability in this situation is that there is at least one point in the domain for which $h_{B_y} h_{0_y} > 0$. We will recover this result again in our treatment of the normal-mode instability problem associated with a parallel shear flow. This result has important implications for the spatial structure of the normal-mode instabilities. In particular, it explains the asymmetrical development of the amplifying perturbation field for an unstable density-driven coupled front (see, for example, Swaters 1991, 1998).

Conditions for nonlinear stability can be established using the functional,

$$\mathcal{L}(\delta \boldsymbol{q}) \equiv \mathcal{H}(\delta \boldsymbol{q} + \boldsymbol{q}_0) - \mathcal{H}(\boldsymbol{q}_0), \tag{2.42}$$

where $\mathcal{H}$ is defined in (2.25), $\boldsymbol{q}_0$ denotes the steady-state solution, $\boldsymbol{q} = \delta \boldsymbol{q} + \boldsymbol{q}_0$ is the total flow field, and $\delta \boldsymbol{q}$ is the finite-amplitude perturbation. We remark that $\mathcal{L}$ is an invariant of the full nonlinear dynamics since each individual functional is. Substituting $\mathcal{H}$ into $\mathcal{L}$ yields

$$
\begin{aligned}
\mathcal{L}(\delta \boldsymbol{q}) = \iiint_\Omega \Big\{ &\tfrac{1}{2}\mu[\nabla \delta\varphi \cdot \nabla \delta\varphi + (\delta\varphi_z/N)^2] \\
&+ \int_{q_{10}}^{q_{10}+\delta q_1} (F_1(\tau) - F_1(q_{10}))\, \mathrm{d}\tau \Big\}\, \mathrm{d}x\mathrm{d}y\mathrm{d}z \\
&+ \iint_{\Omega_H} \Big\{ \Big[N^{-2} \int_{q_{30}}^{q_{30}+\delta q_3} (F_3(\tau) - F_3(q_{30}))\, \mathrm{d}\tau \Big]_{z=-1} \\
&- \Big[N^{-2} \int_{q_{20}}^{q_{20}+\delta q_2} (F_2(\tau) - F_2(q_{20}))\, \mathrm{d}\tau \Big]_{z=0} \\
&- \Big[\int_{q_{40}}^{q_{40}+\delta q_4} (F_4(\tau) - F_4(q_{40}))\, \mathrm{d}\tau \Big] \Big\}\, \mathrm{d}x\mathrm{d}y. \tag{2.43}
\end{aligned}
$$

If we assume that

$$0 < \alpha_i < (-1)^{i+1} F_i' < \beta_i < \infty$$

for all values of the arguments of the F_i' functions, where α_i and β_i are constants, we can derive upper and lower bounds on $\mathcal{L}$, from which we can establish nonlinear stability in the sense of Liapunov with respect to the norm

$$\|\delta\boldsymbol{q}\|^2 \equiv \iiint_\Omega [\nabla\delta\varphi \cdot \nabla\delta\varphi + (\delta\varphi_z/N)^2] + [\delta q_1]^2 \, \mathrm{d}x\mathrm{d}y\mathrm{d}z$$

$$+ \iint_{\Omega_\mathrm{H}} [\delta q_2/N]^2_{z=0} + [\delta q_3/N]^2_{z=-1} + [\delta q_4]^2 \, \mathrm{d}x\mathrm{d}y. \quad (2.44)$$

We now turn to the implication of Andrews's theorem (Andrews 1984) for our results. In practice, we are mostly interested in studying steady solutions in the (non-simply connected) periodic channel (which is useful for shelf dynamics)

$$\Omega = \{(x,y,z), \ -x_\mathrm{B} < x < x_\mathrm{B}, \ 0 < y < L, \ -1 < z < 0\}, \quad (2.45)$$

where the topography is given by $h_\mathrm{B} = h_\mathrm{B}(y)$, the solutions are assumed to be smoothly periodic at $x = \pm x_\mathrm{B}$, and φ is assumed to satisfy appropriate Dirichlet conditions on $y = 0$ and L. It may be viewed as a straightforward extension of Andrews's theorem (Andrews 1984) to show that the only steady solutions for the above channel and topography that can satisfy the linear stability conditions are themselves independent of x, i.e. parallel shear flows.

If we differentiate (2.21)–(2.24) with respect to x, we obtain

$$\mu\varphi_{0_x} = F_{10}'(\triangle\varphi_{0_x} + (\varphi_{0_{xz}}/N^2)_z), \quad (2.46)$$

$$\mu\varphi_{0_x} = F_{20}'(\varphi_{0_{xz}}), \qquad \text{on } z = 0, \quad (2.47)$$

$$\mu\varphi_{0_x} = F_{30}'(\varphi_{0_{xz}} + N^2 h_{0_x}), \qquad \text{on } z = -1, \quad (2.48)$$

$$\mu\varphi_{0_x} = F_{40}'(h_{0_x}), \qquad \text{on } z = -1. \quad (2.49)$$

Multiplying (2.46) by $(\triangle\varphi_{0_x} + (N^{-2}\varphi_{0_{xz}})_z)$, and integrating yields, after a little algebra,

$$\iiint_\Omega \mu[\nabla\varphi_{0_x} \cdot \nabla\varphi_{0_x} + (\varphi_{0_{xz}}/N)^2] + F_{10}'[\triangle\varphi_{0_x} + (\varphi_{0_{xz}}/N^2)_z]^2 \, \mathrm{d}x\mathrm{d}y\mathrm{d}z$$

$$+ \iint_{\Omega_\mathrm{H}} \{F_{30}'[(\varphi_{0_{xz}} + N^2 h_{0_x})/N]^2_{z=-1} - F_{40}'[h_{0_x}]^2 F_{20}'[\varphi_{0_{xz}}/N]^2_{z=0}\} \, \mathrm{d}x\mathrm{d}y = 0.$$

$$(2.50)$$

If we assume that the stability conditions (2.33) hold, it follows from (2.50) that $\varphi_{0_x} = h_{0_x} = 0$, so that only parallel shear flow solutions of the form $\varphi_0(y,z)$ and $h_0(y)$ can, in principle, satisfy the stability conditions for the above channel domain and topographic profile.

Finally, we simply remark that it is possible to give sufficient conditions on the mean flow that establish the analogue of Arnol'd's second linear and nonlinear stability theorems. These conditions amount to establishing the negative definiteness of $\delta^2\mathcal{H}(\varphi_0, h_0)$ and $\mathcal{L}(\delta\boldsymbol{q})$. Because of space considerations here, and the fact that the proof of these results is somewhat more mathematically sophisticated than the arguments just given, we have decided to publish them in full elsewhere (Poulin & Swaters 1999*b*).

3. Linear stability problem

In this section we outline various aspects of the linear stability problem. The presentation is not as general as it can be. For example, we shall restrict our attention to topographic configurations of the form $h_B = h_B(y)$. It is not necessary to do this, and the methods we use will go over to general topographic configurations (see Karsten & Swaters 1996). From a practical point of view, however, this is the topographic configuration most relevant for coastal dynamics.

We also remark that in this section we work with the model equations (1.44)–(1.47) without the (0) superscript. Also, to be concrete, we assume a channel domain given by

$$\Omega = \{(x, y, z), \ 0 < y < L, \ -1 < z < 0\}, \tag{3.1}$$

where we leave unspecified the length of the domain in the x-direction. We remark that we require $\varphi_x = 0$ on $y = 0$ and L, respectively.

Here, we derive the general stability problem for an arbitrary lower-layer thickness profile $h = h_0(y)$ with stable stratification, i.e. $N^2 > 0$. We do not include the possibility of a mean flow in the upper layer. This latter approximation is made in order to focus attention on the purely baroclinic destabilization associated with a lower-layer flow without allowing an unstable mean flow in the upper layer.

Substituting

$$\left. \begin{array}{l} \varphi = \tilde{\varphi}(x, y, t), \\ h = h_0(y) + \tilde{h}(x, y, t) \end{array} \right\} \tag{3.2}$$

into the governing equations, linearizing and dropping the tildes, yields the linear instability problem

$$\triangle\varphi + (N^{-2}\varphi_z)_z = 0, \tag{3.3}$$

$$\varphi_z = 0, \quad \text{on } z = 0, \tag{3.4}$$

$$\varphi_{zt} + N^2 h_{B_y}(\varphi + h)_x = 0, \quad \text{on } z = -1, \tag{3.5}$$

$$h_t - h_{B_y}h_x + \mu h_{0_y}\varphi_x = 0, \quad \text{on } z = -1. \tag{3.6}$$

(a) General linear stability characteristics

It is possible to obtain some general instability properties from the volume-averaged perturbation energy equation, given by

$$\int_{-1}^{0} \int_{0}^{L} \int_{0}^{\lambda} [\triangle\varphi_t + (N^{-2}\varphi_{zt})_z]\varphi \, \mathrm{d}x\mathrm{d}y\mathrm{d}z = 0,$$

which can be rearranged into the form

$$\frac{\partial}{\partial t} \int_{-1}^{0} \int_{0}^{L} \int_{0}^{\lambda} \nabla\varphi \cdot \nabla\varphi + (\varphi_z/N)^2 \, \mathrm{d}x\mathrm{d}y\mathrm{d}z = -2 \int_{0}^{L} \int_{0}^{\lambda} h_{B_y}h\varphi_x \mid_{z=-1} \mathrm{d}x\mathrm{d}y, \tag{3.7}$$

where we have integrated by parts, where necessary exploiting the boundary conditions, and where λ is assumed to be the wavelength of the perturbation in the x-direction, i.e. all perturbation quantities are assumed to be periodic in x with period λ.

The first thing to observe is that if there is no topographic slope, i.e. $h_{B_y} = 0$, then there is no instability (regardless of the shape of $h_0(y)$) since, if $h_{B_y} = 0$, the time rate of change of the perturbation energy, which is a positive definite quadratic functional, is zero. This point makes clear the crucial importance of sloping topography in the instability mechanism modelled here.

(i) *Heat flux associated with an unstable flow*

If we assume instability, then, by definition,

$$\frac{\partial}{\partial t} \int_{-1}^{0} \int_{0}^{L} \int_{0}^{\lambda} \nabla\varphi \cdot \nabla\varphi + (\varphi_z/N)^2 \, \mathrm{d}x\mathrm{d}y\mathrm{d}z > 0, \tag{3.8}$$

which can only be realized if, on average,

$$h_{B_y} h v_1 \big|_{z=-1} < 0. \tag{3.9}$$

If we interpret, for example, a positive h anomaly as a cold or positive mass anomaly in the upper layer, then (3.9) implies that instability can only occur if, on average, there is a net transport of heat in the direction of increasing topographic height (see figure 1), i.e. net anomalous mass transport in the down-slope direction. This is precisely the same situation as in mid-latitude baroclinic instability on a β-plane (see, for example, LeBlond & Mysak 1978; Pedlosky 1987).

(ii) *Sufficient condition for stability*

If we eliminate $\varphi_x \big|_{z=-1}$ in (3.7) using (3.6), we obtain the balance

$$\frac{\partial}{\partial t} \left[\int_{-1}^{0} \int_{0}^{L} \int_{0}^{\lambda} \nabla\varphi \cdot \nabla\varphi + (\varphi_z/N)^2 \, \mathrm{d}x\mathrm{d}y\mathrm{d}z - \int_{0}^{L} \int_{0}^{\lambda} \frac{h_{B_y} h^2}{\mu h_{0_y}} \, \mathrm{d}x\mathrm{d}y \right] = 0, \tag{3.10}$$

where we have integrated by parts once.

Hence, we immediately see again (assuming $N^2 > 0$) that *a sufficient condition for stability is that* $h_{B_y} h_{0_y} < 0$ *for all values of* y and, therefore, *a necessary condition for instability is that there is at least one value of* y *for which* $h_{B_y} h_{0_y} > 0$.

As argued by Swaters (1991, 1998), this necessary condition for instability is important in understanding the lack of symmetry in the spatial structure of the unstable normal-mode instabilities for a coupled front, as predicted by this theory. Consider the situation where $h_{B_y} < 0$, i.e. the mean water depth is increasing in the positive y-direction. The necessary condition for instability is that there exists at least one point for which $h_{0_y} < 0$. For a coupled front, the necessary condition is only satisfied on the down-slope side and is violated on the up-slope side. This asymmetry is a signature of the *baroclinic* instability associated with the model presented here, and can be attributed to the fact that the destabilization occurs due to the release of the gravitational potential energy associated with having a relatively dense pool of water directly sitting on a sloping bottom surrounded by relatively lighter water.

Thus, heuristically, if not rigorously, one expects that the extraction of mean potential energy occurs more efficiently on the down-slope side than on the up-slope side, and this explains why the boundary perturbations on the down-slope side are substantially more pronounced than on the up-slope side (see, for example, Swaters 1991, 1998; Karsten *et al.* 1995).

(iii) *Normal-mode equations*

The normal-mode stability equations are obtained by assuming a solution to (3.3)–(3.6) of the form

$$\varphi = \psi(y, z) \exp[ik(x - ct)] + \text{c.c.}, \tag{3.11}$$

$$h = \eta(y) \exp[ik(x - ct)] + \text{c.c.}, \tag{3.12}$$

yielding

$$(N^{-2}\psi_z)_z + \psi_{yy} - k^2\psi = 0, \tag{3.13}$$

$$\psi_z = 0, \quad \text{on } z = 0, \tag{3.14}$$

$$\psi_z - \frac{N^2 h_{B_y}}{c}\left(1 + \frac{\mu h_{0_y}}{c + h_{B_y}}\right)\psi = 0, \quad \text{on } z = -1, \tag{3.15}$$

$$\eta = \frac{\mu h_{0_y}\psi\,|_{z=-1}}{c + h_{B_y}}, \tag{3.16}$$

where (3.15) and (3.16) have been derived by eliminating η between (3.5) and (3.6).

We now derive the analogue of (3.10) for the normal-mode solutions. If we multiply (3.13) by $c\psi^*$, where ψ^* is the complex conjugate of ψ, and integrate with respect to y and z, we obtain

$$cQ + \int_0^L h_{B_y}\left(1 + \frac{\mu(c^* + h_{B_y})h_{0_y}}{|c + h_{B_y}|^2}\right)|\psi|^2_{z=-1}\,\mathrm{d}y = 0, \tag{3.17}$$

where

$$Q \equiv \int_{-1}^0 \int_0^L N^{-2}|\psi_z|^2 + |\psi_y|^2 + k^2|\psi|^2\,\mathrm{d}y\mathrm{d}z > 0. \tag{3.18}$$

If $c = c_R + ic_I$ is substituted into (3.17), the real and imaginary parts are, respectively,

$$c_R Q + \int_0^L h_{B_y}\left(1 + \frac{\mu(c_R + h_{B_y})h_{0_y}}{|c + h_{B_y}|^2}\right)|\psi|^2_{z=-1}\,\mathrm{d}y = 0. \tag{3.19}$$

$$c_I\left[Q - \int_0^L \frac{\mu h_{B_y}h_{0_y}}{|c + h_{B_y}|^2}|\psi|^2_{z=-1}\,\mathrm{d}y\right] = 0. \tag{3.20}$$

It follows from (3.20) that either $c_I = 0$ (i.e. neutral stability) or the quantity in the square brackets is zero. Thus, again, we see that a requirement for stability is that $h_{B_y}h_{0_y} < 0$ for all y, and that a necessary condition for stability is that there exists at least one value of y for which $h_{B_y}h_{0_y} > 0$.

In the case where the bottom slope is constant it is possible to obtain a simple semicircle theorem. Suppose, without loss of generality, that $h_{B_y} = -1$ (recall that h_B is scaled via its bottom slope) and that instability occurs, it follows from (3.20) that

$$|c - 1|^2 = -\frac{\mu}{Q}\int_0^L h_{0_y}|\psi|^2_{z=-1}\,\mathrm{d}y, \tag{3.21}$$

which if substituted into (3.19) implies

$$\int_0^L |\psi|^2_{z=-1} \, dy = (2c_R - 1)Q. \tag{3.22}$$

However, since we are assuming instability, it follows that

$$\min_{y \in (0,L)} h_{0_y} = -\gamma^2 < 0, \tag{3.23}$$

which, together with (3.21) and (3.22), implies

$$|c - 1|^2 \leqslant \frac{\mu\gamma^2}{Q} \int_0^L |\psi|^2_{z=-1} \, dy = \mu\gamma^2(2c_R - 1),$$

which can be rearranged into the form

$$(c_R - 1 - \mu\gamma^2)^2 + c_I^2 \leqslant \mu\gamma^2(1 + \mu\gamma^2). \tag{3.24}$$

(b) Linear stability problem for a simple wedge front

The linear stability problem (3.13)–(3.15) is not separable and, thus, analytical solutions, in general, cannot be obtained, and a numerical solution is required. However, for the extremely simple configuration consisting of an unsheared gravity current flowing along a constant sloping bottom, the linear stability problem can be solved exactly. While perhaps far too simple to have any practical value, this solution is, nevertheless, instructive in illustrating several important dynamical points.

Let us assume

$$h_0 = 1 - \gamma y/\mu \quad (\gamma > 0) \text{ and } h_B = -y. \tag{3.25}$$

Substituting (3.25) into (3.13)–(3.15) yields

$$\phi_{zz} - \lambda^2 \phi = 0, \tag{3.26}$$

$$\phi_z = 0, \quad \text{on } z = 0, \tag{3.27}$$

$$\phi_z + \frac{N^2}{c}\left(1 + \frac{\gamma}{1-c}\right)\phi = 0, \quad \text{on } z = -1, \tag{3.28}$$

where we have assumed

$$\psi(y, z) = \sin([n\pi y]/L)\phi(z), \tag{3.29}$$

$$\lambda^2 \equiv N^2(k^2 + ([n^2\pi^2]/L^2)), \tag{3.30}$$

and a constant Brunt–Väisälä frequency.

The solution is given by

$$\phi = A\cosh(\lambda z), \tag{3.31}$$

with the dispersion relationship

$$c = \frac{\lambda T + N^2 \pm \sqrt{(\lambda T - N^2)^2 - 4\gamma\lambda T N^2}}{2\lambda T}, \tag{3.32}$$

where $T \equiv \tanh(\lambda)$, and where A is a free amplitude parameter. It is straightforward to verify that in the limit $N \to 0$, equation (3.32) reduces exactly to the two-layer result presented in Mooney & Swaters (1996).
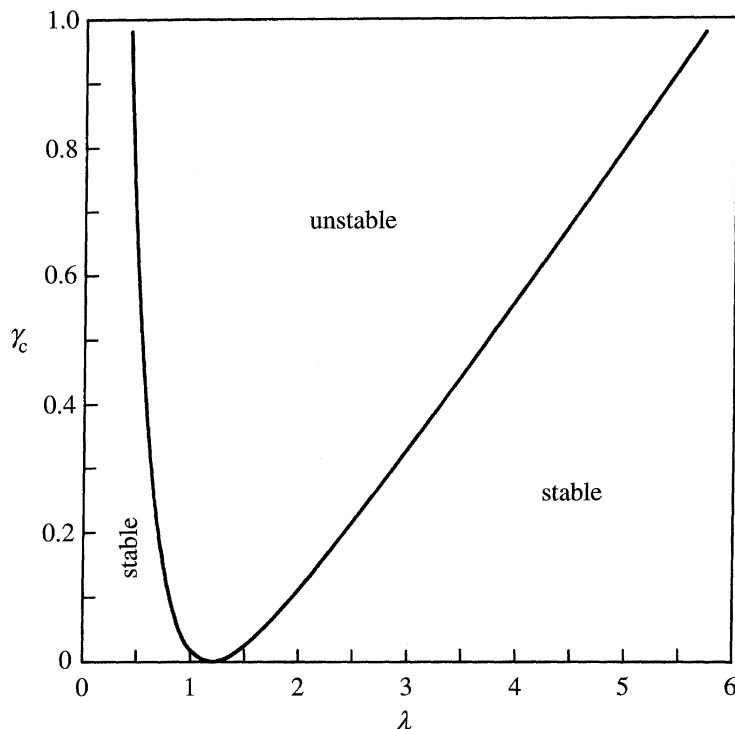
Figure 2. The marginal stability curve in (λ, γ) coordinates with the linearly sloping frontal profile (3.25) with $N = 1.0$.

The marginal stability curve, denoted as $\gamma_c = \gamma_c(\lambda)$, is given by

$$\gamma_c = \frac{(\lambda T - N^2)^2}{4\lambda T N^2},\qquad(3.33)$$

with the unstable region in (k, γ) parameter space given by $\gamma > \gamma_c$. In figure 2 we plot γ_c versus λ for $N = 1.0$.

The point of marginal stability is determined by

$$\frac{\partial \gamma_c(k_m)}{\partial k} = 0.\qquad(3.34)$$

For sufficiently wide domains, the point of marginal stability will be given by

$$\gamma_m \equiv \gamma_c(k_m) = 0,\qquad(3.35)$$

with wavenumber k_m determined by solving for λ_m from

$$\lambda_m \tanh(\lambda_m) = N^2,\qquad(3.36)$$

which has a real $k_m \geqslant 0$ solution only if $L \geqslant N\pi/\lambda_m$. It is straightforward to check that as $L \to (N\pi/\lambda_m)^+$, $k_m \to 0^+$. For narrow domains, i.e. those for which $L < N\pi/\lambda_m$, it follows from (3.34) that $k_m = 0$ and $\gamma_m > 0$. Thus we see that k_m is a continuous function of L. From our point of view, the large L limit is most applicable since it seems more appropriate for continental shelf dynamics.

We can determine the interval of unstable wavenumbers for a given γ. It follows from (3.32) that instability occurs when

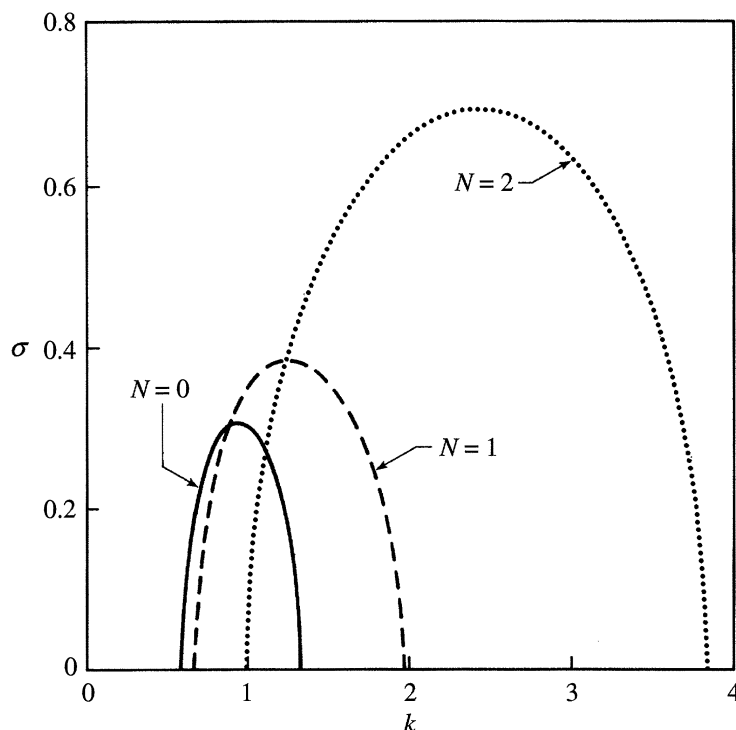$$(\lambda T - N^2)^2 - 4\gamma \lambda T N^2 < 0,\qquad(3.37)$$

Figure 3. The growth rate σ versus the along-slope wavenumber k for the gravest cross-channel mode associated with the unstable linearly sloping frontal profile (3.25) for $N = 0.0$, 1.0 and 2.0, respectively.

which can be rearranged into the form

$$\frac{1}{1 + 2\gamma + 2\sqrt{\gamma(1 + \gamma)}} < \frac{\lambda T}{N^2} < 1 + 2\gamma + 2\sqrt{\gamma(1 + \gamma)}. \qquad (3.38)$$

Thus, we see that we have a high *and* low wavenumber cut-offs. Thus, in the limit $\gamma^2 \to 0$, the flow becomes stable as it must. Although not a general result, this property is important because it suggests that the present model avoids the ultraviolet catastrophe that occurs in many planetary geostrophic models (see, for example, Pedlosky 1984; de Verdiere 1986) and, therefore, that the most unstable mode will not occur at a wavenumber that violates the underlying asymptotic assumptions of the model.

From (3.38), we see that as N increases, the length of the interval of unstable wavenumbers increases and is shifted to higher along-channel wavenumbers. In figure 3 we plot the growth rate, $\sigma = kc_I$ versus k for the gravest cross-channel mode $n = 1$ for $N = 0.0$, 1.0 and 2.0, respectively. The blue shift associated with increasing N is evident. We also see that growth rate and along-slope wavenumber of the most unstable mode monotonically increases with increasing N.

Finally, we remark that the $\gamma = 0$ solutions are simply f-plane neutral bottom-trapped topographic Rossby waves as described, for example, by Rhines (1970) or LeBlond & Mysak (1978, §20). Thus, from a modal point of view, the instability is the result of the coalescence of two neutral topographic Rossby waves (see also Mooney & Swaters 1996; Boss *et al.* 1996).

4. Conclusions

Our principal focus in this paper has been to introduce and qualitatively analyse a new model that describes the sub-inertial dynamics of density-driven currents within a continuously stratified fluid of finite depth overlying a sloping bottom. In order to differentiate these flows from their non-rotating counterparts, we refer to them as mesoscale gravity currents.

The model we develop was obtained as a formal asymptotic reduction of a two-fluid system. The upper fluid is continuously stratified and is described by baroclinic QG dynamics in which the Eulerian velocity field is principally driven by vortex tube stretching/compression associated with the deforming interface between the upper layer and the mesoscale gravity current and a topographic background vorticity gradient. The lower layer, i.e. the density-driven current, is assumed to be homogeneous, and is modelled as a geostrophically balanced flow, which allows finite-amplitude thickness variations. The two layers are strongly coupled together. This model filtered out barotropic instabilities in the gravity current focused on the baroclinic destabilization of these flows.

This model possessed an underlying Hamiltonian formulation and this structure was exploited to develop general linear and nonlinear criteria for steady solutions. The linear stability problem was examined in some detail. In particular, we showed that a necessary condition for instability was that there was net offshore transport of mass anomalies in the overlying fluid.

This necessary condition for instability results in the asymmetrical development of perturbations on the down-slope side for a coupled-front lower-layer thickness profile. Numerical simulations based on a two-layer analogue of the present model (Swaters 1998) have suggested that these down-slope perturbations develop into down-slope-propagating plumes, which can subsequently evolve into along-slope propagating cold domes.

We were also able to derive a semicircle theorem for the general normal-mode instability problem. The instability characteristics are illustrated by solving the normal-mode instability equations for an unsheared gravity current configuration. It is shown that the range of unstable wavenumbers is shifted upscale with increasing stratification in the upper layer. We also showed that the growth rate and wavenumber of the most unstable mode increases with increasing stratification in the overlying layer.

While, in this paper, a major objective has been to study the stability characteristics of the model, in part II we examine eddy solutions to the model. In particular, we give a variational principle for steadily travelling solutions. We also construct explicit solutions for an isolated eddy solution and present an asymptotic solution for a radiating cold dome.

References

Andrews, D. G. 1984 On the existence of nonzonal flows satisfying sufficient conditions for stability. *Geophys. Astrophys. Fluid Dynamics* **28**, 243–256.

Benjamin, T. B. 1984 Impulse, flow force and variational principles. *IMA J. Appl. Math.* **32**, 3–68.

Boss, E., Paldor, N. & Thompson, L. 1996 Stability of a potential vorticity front: from quasi-geostrophy to shallow water. *J. Fluid Mech.* **315**, 65–84.

Britter, R. E. & Linden, P. F. 1980 The motion of the front of a gravity current travelling down an incline. *J. Fluid Mech.* **99**, 531–543.

Bruce, J. G. 1995 Eddies southwest of the Denmark Strait. *Deep Sea Res.* **42**, 13–29.

Chapman, D. C. & Gawarkiewicz, G. 1995 Offshore transport of dense shelf water in the presence of a submarine canyon. *J. Geophys. Res.* **100**, 13 373–13 387.

Charney, J. G. & Flierl, G. R. 1981 Oceanic analogues of large-scale atmospheric motion. In *Evolution of physical oceanography—scientific surveys in honor of Henry Stommel* (ed. B. A. Warren & C. Wunsch), pp. 504–548. Cambridge, MA: MIT Press.

de Verdiere, A. C. 1986 On mean flow instabilities within the planetary geostrophic equations. *J. Phys. Oceanogr.* **16**, 1981–1984.

Gawarkiewicz, G. & Chapman, D. C. 1995 A numerical study of dense water formation and transport on a shallow, sloping continental shelf. *J. Geophys. Res.* **100**, 4489–4507.

Griffiths, R. W., Killworth, P. D. & Stern, M. E. 1982 Ageostrophic instability of ocean currents. *J. Fluid Mech.* **117**, 343–377.

Holm, D. D. 1985 Hamiltonian formulation of the baroclinic quasi-geostrophic fluid equations. *Phys. Fluids* **29**, 7–8.

Holm, D. D., Marsden, J. E., Ratiu, T. & Weinstein, A. 1985 Nonlinear stability of fluid and plasma equilibria. *Phys. Rep.* **123**, 1–116.

Honji, H. & Hosoyamada, T. 1989 Instability of the rotating gravity current flow down a slope. *Rep. Res. Inst. Appl. Mech.* **35**, 55–64.

Houghton, R. W., Schlitz, R., Beardsley, R. C., Butman, B. & Chamberlin, J. C. 1982 The middle Atlantic bight pool: evolution of the temperature structure during 1979. *J. Phys. Oceanogr.* **25**, 1019–1029.

Jiang, L. & Garwood Jr, R. W. 1995 A numerical study of three-dimensional dense bottom plumes on a Southern Ocean continental slope. *J. Geophys. Res.* **100**, 18 471–18 488.

Jiang, L. & Garwood Jr, R. W. 1996 Three-dimensional simulations of overflows on continental slopes. *J. Phys. Oceanogr.* **26**, 1214–1233.

Karsten, R. H. & Swaters, G. E. 1996 Nonlinear stability of baroclinic fronts in a channel with variable topography. *Stud. Appl. Math.* **96**, 183–199.

Karsten, R. H., Swaters, G. E. & Thomson, R. E. 1995 Stability characteristics of deep-water replacement in the Strait of Georgia. *J. Phys. Oceanogr.* **25**, 2391–2403.

Killworth, P. D. 1977 Mixing on the Weddell Sea continental slope. *Deep Sea Res.* **24**, 427–488.

LeBlond, P. H. & Mysak, L. A. 1978 *Waves in the ocean.* Elsevier.

LeBlond, P. H., Ma, H., Doherty, F. & Pond, S. 1991 Deep and intermediate water replacement in the Strait of Georgia. *Atmos. Ocean* **29**, 288–312.

Melling, H. & Lewis, E. L. 1982 Shelf drainage flows in the Beaufort Sea and their effect on the Arctic Ocean pycnocline. *Deep Sea Res.* **29**, 967–985.

Mooney, C. J. & Swaters, G. E. 1996 Finite-amplitude baroclinic instability of a mesoscale gravity current in a channel. *Geophys. Astrophys. Fluid Dynamics* **82**, 173–205.

Morrison, P. J. 1982 Poisson brackets for fluids and plasmas. In *Mathematical methods in hydrodynamics and integrability in dynamical systems* (ed. M. Tabor & Y. M. Treve). *AIP Conf. Proc.*, vol. 88, pp. 13–46.

Nof, D. 1983 The translation of isolated cold eddies on a sloping bottom. *Deep Sea Res.* **30**, 171–182.

Olver, P. J. 1982 A nonlinear Hamiltonian structure for the Euler equations. *J. Appl. Math. Analysis* **89**, 233–250.

Pedlosky, J. 1984 The equations for geostrophic flow in the ocean. *J. Phys. Oceanogr.* **14**, 448–455.

Pedlosky, J. 1987 *Geophysical fluid dynamics.* Springer.

Poulin, F. J. 1997 Mesoscale gravity currents and cold-pools within a continuously-stratified fluid overlying gently sloping topography. MSc thesis, Department of Mathematical Sciences, University of Alberta.

Poulin, F. J. & Swaters, G. E. 1999a Sub-inertial dynamics of density-driven flows in a continuously stratified fluid on a sloping bottom. II. Isolated eddies and radiating cold domes. *Proc. R. Soc. Lond.* A **455**, 2305–2329. (Following paper.)

Poulin, F. J. & Swaters, G. E. 1999b Sub-inertial dynamics of density-driven flows in a continuously stratified fluid on a sloping bottom. III. Nonlinear stability theory. *Can. Appl. Math. Quart.* **7**, 49–69.

Price, J. & Baringer, M. O. 1994 Outflows and deep water production by marginal seas. *Prog. Oceanogr.* **33**, 161–200.

Rhines, P. B. 1970 Edge-, bottom, and Rossby waves in a rotating stratified fluid. *Geophys. Fluid Dynamics* **1**, 273–302.

Shapiro, G. I. & Hill, A. E. 1997 Dynamics of dense water cascades at the shelf edge. *J. Phys. Oceanogr.* **27**, 2381–2394.

Shepherd, T. G. 1990 Symmetries, conservation laws, and Hamiltonian structure in geophysical fluid dynamics. *Adv. Geophys.* **32**, 287–335.

Smith, P. C. 1975 A streamtube model for bottom boundary currents in the ocean. *Deep Sea Res.* **22**, 853–973.

Smith, P. C. 1976 Baroclinic instability in the Denmark Strait overflow. *J. Phys. Oceanogr.* **6**, 355–371.

Speer, K., Tziperman, E. & Feliks, Y. 1993 Topography and grounding in a simple bottom layer model. *J. Geophys. Res.* **98**, 8547–8558.

Steacy, M. W., Pond, S. & LeBlond, P. H. 1988 An objective analysis of the low-frequency currents in the Strait of Georgia. *Atmos. Ocean* **26**, 1–15.

Swaters, G. E. 1985 A nonlinear stability theorem for baroclinic quasigeostrophic flow. *Phys. Fluids* **29**, 5–6.

Swaters, G. E. 1991 On the baroclinic instability of cold-core coupled density fronts on a sloping continental shelf. *J. Fluid Mech.* **224**, 361–382.

Swaters, G. E. 1993 Nonlinear stability of intermediate baroclinic flow on a sloping bottom. *Proc. R. Soc. Lond.* A **442**, 249–272.

Swaters, G. E. 1998 Numerical simulations of the baroclinic dynamics of density-driven coupled fronts and eddies on a sloping bottom. *J. Geophys. Res.* **103**, 2945–2961.

Swaters, G. E. & Flierl, G. R. 1991 Dynamics of ventilated coherent cold eddies on a sloping bottom. *J. Fluid Mech.* **223**, 565–587.

Whitehead, J. A. & Worthington, L. U. 1982 The flux and mixing rates of Antarctic Bottom Water within the North Atlantic. *J. Geophys. Res.* **87**, 7903–7924.

Zoccolotti, L. & Salusti, E. 1987 Observations on a very dense marine water in the Southern Adriatic Sea. *Continent. Shelf Res.* **7**, 535–551.